Comparison of shear wave velocity calculation techniques for centrifuge test data

D.M. Xu, S.S.W. Weerasuriya Achchillage, and S.P.G. Madabhushi
University of Cambridge, Cambridge, United Kingdom, dmx20@cam.ac.uk, ssww2@cam.ac.uk, mspg1@cam.ac.uk

ABSTRACT: The method of measuring the propagation of shear wave velocity through a soil column to determine the small strain stiffness is commonplace for centrifuge models. An "air hammer" device sends shear waves through the soil in flight and are picked up by a vertical array of accelerometers. There are different methods to calculate the time delay for the shear wave to reach each accelerometer, which results in different wave speeds and soil stiffness. This paper explores the advantages and disadvantages of two such methods: peak to peak, where a single peak is considered, and cross correlation, where the entire shear wave is considered. To compare the two methods, MATLAB code was written to use *findpeaks* and *xcorr* to calculate and plot wave speed from centrifuge test data. Good agreement is achieved in ideal conditions, but other situations where each method is superior, and should be used, or a pitfall, giving unreliable results, are presented and discussed.

1 INTRODUCTION

One important part of the data collection from a dynamic centrifuge test are the accelerations. This includes the input motion from the simulated earthquake, the model's corresponding reaction, but is also a way to characterise the soil profile.

Piezoelectric (PE) sensors, based off of the charge released by a piezoelectric crystal under stress, were the first accelerometers to be used in the centrifuge (Morris, 1979). Another type of accelerometer currently in use is the MEMS (micro-electrical-mechanical-system) sensor (Stringer et al., 2010). These have a very small suspended mass at the centre, when acceleration occurs, this mass shifts, changing the capacitance of various sensing "fingers". MEMS accelerometers have the advantage of being able to record both static and dynamic acceleration, but are also physically smaller than their PE counterparts (5 mm × 5 mm × 2 mm compared to 10 mm × 10 mm × 10 mm), this is of particular importance due to the centrifuge scaling laws laid out by Schofield (1980).

To characterise the soil profile in flight, Ghosh and Madabhushi (2002) presented an air hammer device, which, when powered with compressed air, generate shear waves that propagate through the soil model. The shear wave velocity (V_s) can be measured using a column of embedded accelerometers, when combined with the bulk density of the soil (ρ) as shown in Equation 1, one can calculate the maximum low strain shear modulus (G_{max}).

$$G_{max} = \rho \cdot V_s^2 \qquad (1)$$

The shear wave velocity is predominantly a function of the soil voids ratio, with any changes in the measurement alone being a clear sign of changes to the soil property over time. Alternate soil characterisation methods include the CPT or SPT, though both are more difficult to perform in flight, but do provide continuous data with respect to depth. In contrast, a limitation of the air hammer method is that two sensors placed apart are required to measure each discrete shear wave velocity, though soil compressibility has very little effect on measurements, while it has a large effect on CPT and SPT data. In addition, CPT and SPT data often rely on empirical correlations to calculate soil properties.

There has been limited studies published on shear wave velocity measurements in the centrifuge, and none covering the methods to calculate wave speeds from raw data. Gohl and Finn (1987) placed bender elements in a model of dry sand to generate and capture shear waves, while Kita et al. (1996) used a similar methodology for Kaolin clay. More recently, Arulnathan et al. (2000) discussed the usage of an air hammer device at UC Davis.

This paper first describes the air hammer device used at the University of Cambridge, along with an example sand model for context. While the method of using an air hammer to characterise clay soils also exists, for the purpose of this paper, only sand model data is discussed. Next, some results comparing two methods of calculating shear wave velocity from acceleration time history data are discussed.

2 OVERVIEW OF METHODOLOGY

2.1 Air hammer device

The air hammer device consists of an 80 mm long, 10 mm diameter brass tube, within which a shuttle resides. The outside of the brass tube is made rough, to ensure proper coupling with the soil body, by coating it in a mixture of two-part epoxy resin and coarse sand. The shuttle is a length of steel rod (for mass), with two PTFE end caps to ensure the shuttle runs smoothly within the brass housing.

Compressed air is pushed into alternate ends of the air hammer device by a three-way valve. With each air injection, the shuttle is moved and hits the end of the device, this creates the shear wave. Figure 1 shows both a photograph of the device placed at the bottom of a model strongbox, and also a schematic of the device. The device is able to operate with either compressed air, or under vacuum, which has the advantage of not leaking air into sensitive models if there is a leak.

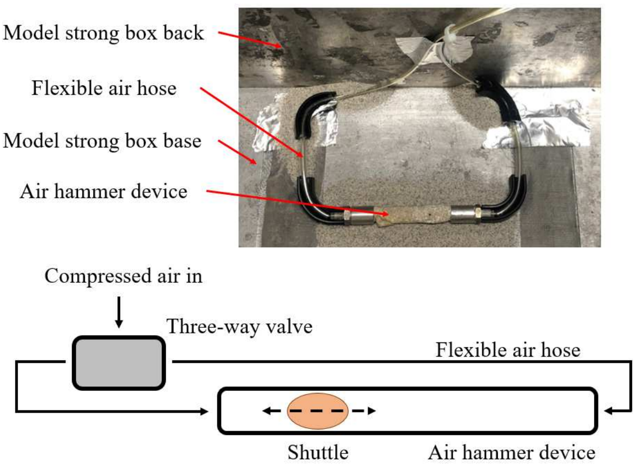

Figure 1. Photograph of an air hammer device in a model strongbox, and a schematic showing the functioning of the device.

The air hammer was designed to minimise P wave generation (by reducing the contact area between soil and hammer) and to produce a S wave that is both small enough to not disturb loose sand models, but clear enough to be detected by accelerometers to make subsequent data analysis meaningful.

In these example centrifuge tests, the air hammer is placed at the bottom of the model, with the shear wave propagating from the bottom to the surface of the soil model. Conversely, one can place the air hammer device at the top of the model, this is often done with clay models due to the limitations imposed on the model making process as the clay needs to be consolidated. For sand models, at lower g levels, there is better coupling between the hammer and soil if the device is placed at the bottom.

2.2 Centrifuge model

An example dynamic model schematic is shown in Figure 2. Only the air hammer device and accelerometer locations and sensor IDs are shown, in reality, other sensors such as pore pressure transducers were present, but are outside the scope of this paper. Two accelerometers (for redundancy) are also included on the model strongbox to record the earthquake input motion, again, these data are not analysed for the air hammer and soil profile.

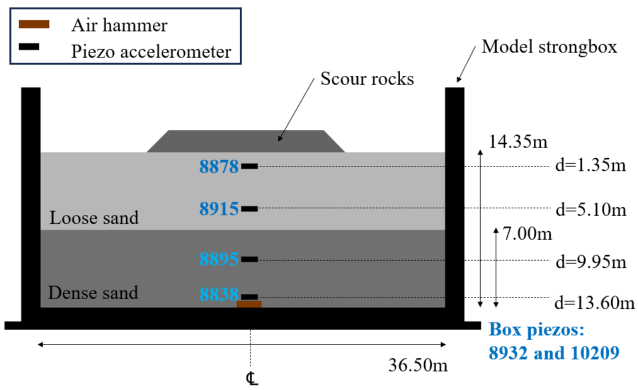

Figure 2. Simplified test schematic adapted from Xu et al., (2025) showing accelerometer positions and IDs.

The model was constructed to study the seismic behaviour of scour protection rock berms for the offshore wind industry (Xu et al., 2023), but serves as a good model to study the calculation of shear wave speed from raw centrifuge data.

The model was made using Hostun HN31 sand, whose physical parameters are presented in Table 1. Loose and dense sand have a relative density of 46 and 90% respectively. The sand was poured into the model strongbox, measuring 730 mm × 250 mm × 400 mm, using an automatic sand pouring machine (Madabhushi et al., 2006), and saturated under vacuum using a Raspberry Pi controlled system that is an updated version of the “Cam Sat” system (Stringer and Madabhushi, 2009).

During a centrifuge test, air hammer tests are carried out during swing up, at incremental g levels, and again before and after each earthquake (earthquakes applied using the servo-hydraulic shaker (Madabhushi et al., 2012)), though for this paper, only a few data sets are needed to illustrate the wave speed calculation.

Table 1. Properties of Hostun HN31 sand.

Property	Value	Units
D_{10} grain size	0.230	mm
D_{50} grain size	0.325	mm
D_{60} grain size	0.353	mm
Specific gravity (G_s)	2.65	-
Minimum voids ratio (e_{min})	0.555	-
Maximum voids ration (e_{max})	1.010	-
Critical angle of friction (φ_{crit})	34.6	°
Coefficient of uniformity (C_u)	1.57	-

2.3 Data acquisition

Shear wave velocity through sand is around 200 m/s, the model is 280 mm deep at model scale, this means the data logging rate needs to be very high to capture the time delay of the shear wave from sensor to sensor.

DASYLab v13.0 was used to log data into text files for later processing, these files contain time and voltage data. For air hammer accelerations, the logging rate used was 30,000 Hz. Raw sensor voltages are calibrated against sensor calibration factors in MATLAB R2019b using a bespoke script called *CaliPlot*.

3 MATLAB CODE AND DISCUSSION

3.1 MATLAB code

MATLAB code was written in R2019b to take the output of *CaliPlot* (prototype scale acceleration time histories) to calculate shear wave speed. Options coded included:

- Wave speed calculation using *findpeaks*, *xcorr*, or both methods.
- Calculate wave speed between only successive senor pairs or all sensor pair combinations (e.g. wave speed between shallowest and deepest sensor, skipping middle sensors).
- Include or exclude negative wave speeds caused by erroneous data.
- Show or omit sensor ID labels on result plots.

3.2 Wave speed calculation methods

The two methods of wave speed calculation chosen are *findpeaks* and *xcorr*. These two methods cover the most common two types of methods employed.

The method of *findpeaks* allows the user to set parameters for MATLAB to automatically detect and select a specific peak within each sensor's signal. The time of the selected peak is then compared between sensors to calculate the time delay, and thus the wave speed. The most common method is to use the first significant wave; this avoids using the smaller waves within the waveform that may have attenuation or dispersive errors. Another option is to use the global maximum wave in terms of amplitude. Here, the first significant wave is used.

The method of *xcorr* compares the entire signal, rather than the time instance of a specific wave, using the cross-correlation function. The similarity between two signals is calculated by sliding one over the other and calculating the sum of their products at every possible overlap position. The peak of the sum of products will reveal the time delay between the two signals.

When using either method, a 0.5 second snippet (Figure 3) of the complete recorded data, that contains a single air hammer shear wave, is used as the sensor signal (the snippet length can be adjusted to suit the specific use case to crop out potential noise). The snippet is found using the global maximum of the deepest sensor signal. This is required for *xcorr*, rather than using multiple shear waves, as 3 to 4 are usually recorded, but used for *findpeaks* as well for consistency.

3.3 Wave speed calculation of ideal data

Ideal acceleration data was used to identify differences between the two calculation methods. Figure 3 shows the 0.5 second snippet of the acceleration time history, at prototype scale. The sensor ID (corresponding to Figure 2), depth, minimum and maximum readings are included, and the red star marks the location of the peak used by *findpeaks* for each signal.

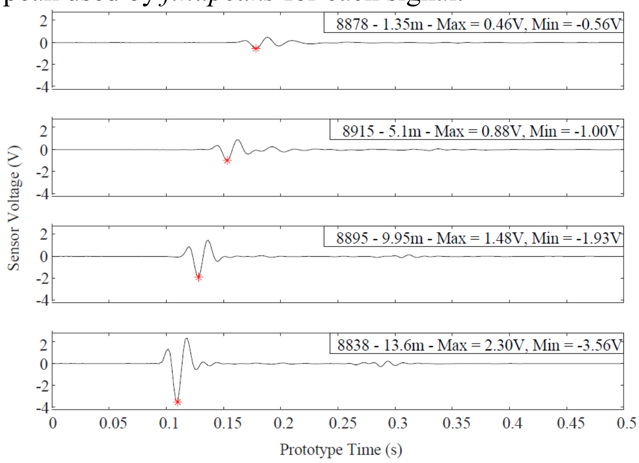

Figure 3. Prototype acceleration time history of ideal data, with findpeaks selected peaks in red.

In this case, the signals are clean, with the first significant peak also being the maximum peak, there is also a clear time delay from the deepest to the shallowest sensor. Figure 4 shows the calculated wave speeds, with *findpeaks* in black, and *xcorr* in blue, all wave speeds between all sensor pairs are plotted.

It can be seen that the two methods produce the same wave speeds (red data points) that agree with empirical data by both Hardin and Drenvich (1972), and Oztoprak and Bolton (2013). These results are only identical if there are enough sensors spread across the depth of the model. The data points where all sensor pairs are considered (non-red data points) show a difference in the computed speeds, even for ideal data. As the signal attenuates and disperse, travelling from the bottom of the model to the top, the calculations made by the two methods start to differ. The peak-to-peak difference is smaller than the if the entire waveform is considered, as the waveform shape and spread begins to change as the signal travels upwards, hence the *xcorr* data points (blue crosses) where sensor to sensor distance is increased, is 2 to 3% lower.

Taking the *findpeaks* case in Figure 5, it can be seen that taking sensors further apart and calculating the wave speed across a longer distance will produce results that are different to that from successive sensors, this is because the wave speed changes with depth. This change is more rapid at shallower depths, hence the closer agreement between the black and red triangles at depths >8 m.

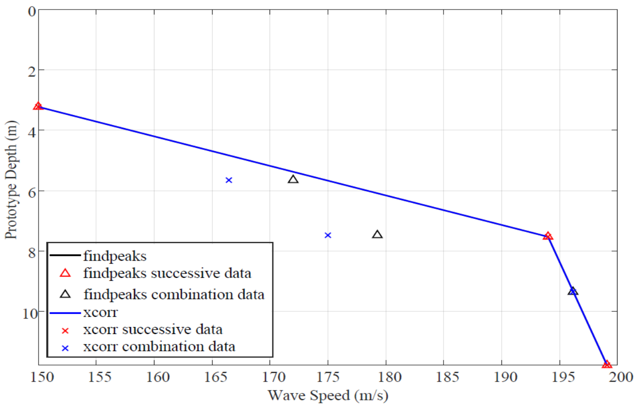

Figure 4. Calculated wave speeds using findpeaks (black) and xcorr (blue). Red data points are from successive sensors.

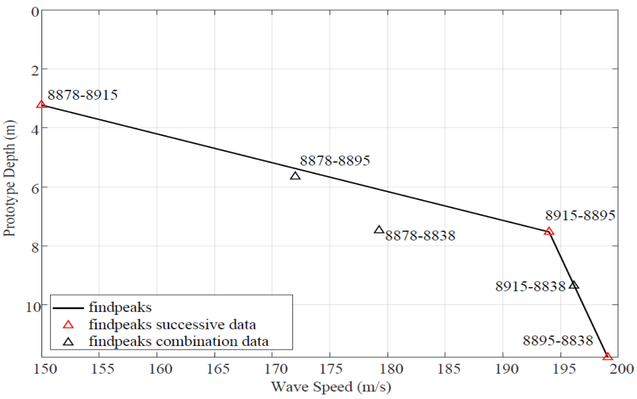

Figure 5. Calculated wave speeds using findpeaks with sensor ID labels, all sensor pairings shown.

3.4 Wave speed calculation of non-ideal data

Non-ideal data was used to study cases when each method should be used, with examples provided below. The acceleration time histories shown in Figure 6 are from a different test flight, this time it can be seen that *findpeaks* is in fact picking an incorrect first significant peak (sensor 8880). Looking at the wave speed calculation results in Figure 7 shows that *xcorr* is the preferred method in this case, giving more reliable values of wave speed, as the entire waveform is considered, not just the time of a specific peak.

It is noted that the soil profile for this section is 14.35 m of loose sand, and that the magnitude of the acceleration signals change between each example in this paper, this is because the *g* level is changing, and all plots are at prototype scale, though this does not affect the shear wave speed calculations, only that specific data have been chosen to illustrate the strengths and weaknesses of each calculation method.

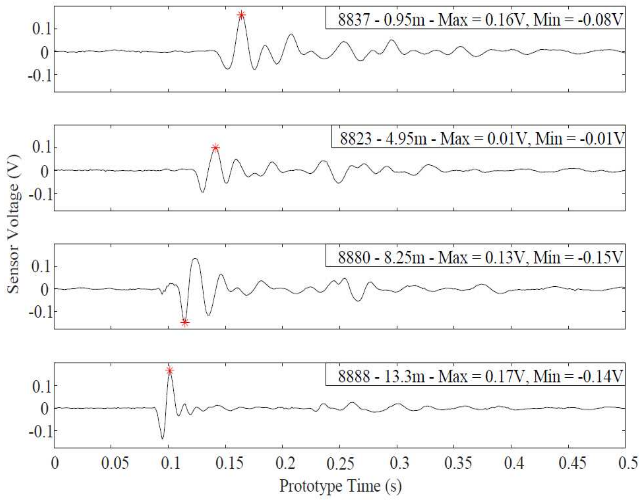

Figure 6. Prototype acceleration time history of non-ideal data, with findpeaks selected peaks in red.

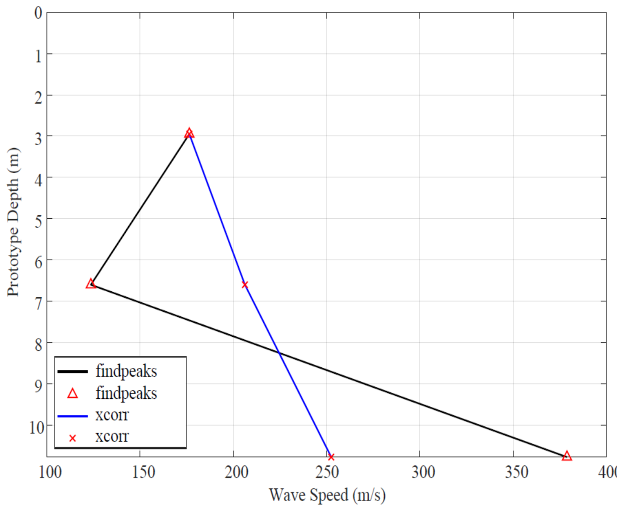

Figure 7. Calculated wave speeds using findpeaks (black) and xcorr (blue) from successive sensors.

The same model is presented in Figure 8. This time, due to the model being only at 20 *g*, the waveform's shape changes from sensor to sensor due to a lack of soil coupling. In this case, using *findpeaks* will give more realistic wave speeds compared to *xcorr* which tries to match the entire waveform, as shown in Figure 9 (typical wave speeds, depending on the sand and packing density, do not exceed 400m/s).

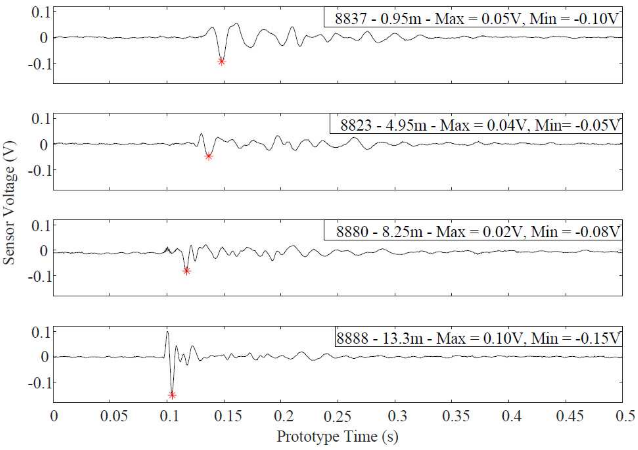

Figure 8. Prototype acceleration time history of non-ideal data, with findpeaks selected peaks in red.

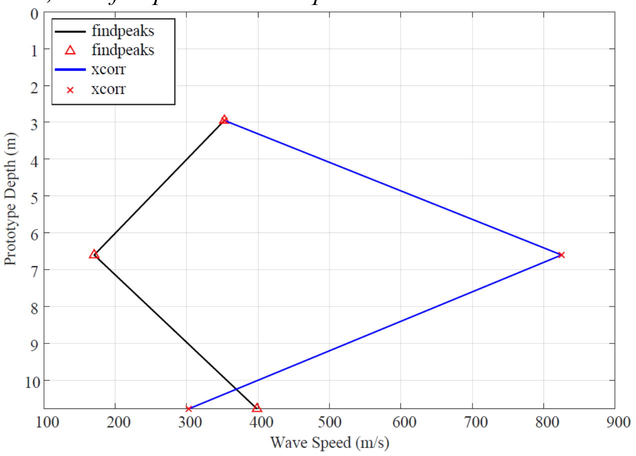

Figure 9. Calculated wave speeds using findpeaks (black) and xcorr (blue) from successive sensors.

4 CONCLUSIONS

This paper has presented an overview of the use of air hammer devices in dynamic centrifuge testing as a means of characterising the soil profile.

MATLAB code was written to calculate wave speeds from acceleration time histories using *findpeaks*, which uses the time delay between the first significant peak, and *xcorr*, with uses the cross correlation between two complete signals to calculate the time delay.

Differences are seen between the two methods, and examples of where each method is preferable are also presented. To summarise:

- The calculated shear wave velocities show good agreement to both Hardin and Drenvich (1972), and Oztoprak and Bolton (2013).
- Using ideal acceleration data, both *findpeaks* and *xcorr* will calculate the same shear wave velocities, as long as there are enough sensors spread across the depth of the model.
- Shallower regions will have higher differences in wave speed across different calculation methods and sensor pairings used, as the rate of change in wave speed through the soil is higher than in deeper parts of the model.
- *xcorr* should be used when sensor waveform shapes match, this avoids the potential of *findpeaks* targeting the wrong peak.
- *findpeaks* should be used instead when the sensor signals do not match, for example due to low *g* level soil coupling, *xcorr* will throw out unrealistic wave speeds.

Both methods discussed can provide reliable shear wave speed calculations, but care should always be taken to examine the sensor signals prior to any calculations, to avoid potential errors as shown above, and verify results.

REFERENCES

Arulnathan, R. & Boulanger, R. W, Kutter, B.L and Sluis, W.K. (2000). New tool for shear wave velocity measurements in model tests. *Geotechnical testing journal*, 23(4): 444–453. https://doi.org/10.1520/GTJ11065J

Ghosh B. and Madabhushi, S.P.G. (2002). An efficient tool for measuring shear wave velocity in the centrifuge. *Physical Modelling in Geotechnics: Proceedings of the International Conference ICPMG '02*, 1st ed., Taylor & Francis Group, pp. 119–124. https://doi.org/10.1201/9780203743362-21

Gohl, W.B. and Finn, W.D.L. (1987). Seismic response of pile foundation in a centrifuge. *Proceedings of international symposium and Prediction and Performance in Geotechnical Engineer,* Balkema, pp. 419–426.

Hardin, B.O., and Drnevich, V.P. (1972). Shear modulus and damping in soils: Design equations and curves. *Journal of the Soil Mechanics and Foundations Division*, 98(7): 667–692. https://doi.org/10.1061/JSFEAQ.0001760

Kita, K., Shibata, T.,Yashima, A., and Kobayashi,S. (1992). Measurement of shear wave velocities of sand in a centrifuge. *Journal of Soils and Foundation,* 32(2): 134–140. https://doi.org/10.3208/sandf1972.32.2_134

Madabhushi, S.P.G., Houghton, N.E., Haigh, S.K. (2006). A new automatic sand pourer for model preparation at University of Cambridge. *Proceedings of the 6th International Conference on Physical Modelling in*

Geotechnics, Taylor & Francis Group, pp. 217–222. https://doi.org/10.1201/noe0415415866.ch25

Madabhushi, S.P.G., Haigh, S.K., Houghton, N.E., and Gould, E. (2012). Development of a servo-hydraulic earthquake actuator for the Cambridge Turner beam centrifuge. *International Journal of Physical Modelling in Geotechnics,* 12(2): 77–88. https://doi.org/10.1680/ijpmg.11.00013

Morris, D.M. (1979). The centrifugal modelling of dynamic behaviour. University of Cambridge, UK.

Oztoprak, S. and Bolton, M.D. (2013). Stiffness of sand through a laboratory test database. *Géotechnique*, 63(1): 54–70. https://doi.org/10.1680/geot.10.P.078

Schofield, A.N. (1980). Cambridge Geotechnical Centrifuge Operations. *Géotechnique*, 30(3): 227–268.

Stringer, M.E. and Madabhushi, S.P.G. (2009). Novel computer-controlled saturation of dynamic centrifuge models using high viscosity fluids. *Geotechnical Testing Journal,* 32(6): 559–564. https://doi.org/10.1520/GTJ102435

Stringer, M.E., Heron, C.M., and Madabhushi, S.P.G. (2010). Experience using MEMS-based accelerometers in dynamic testing. *Physical Modelling in Geotechnics, Two Volume Set: Proceedings of the 7th International Conference on Physical Modelling in Geotechnics (ICPMG 2010)*, 1st ed., Taylor & Francis Group, pp. 389–394. https://doi.org/10.1201/b10554

Xu, D.M., Madabhushi, S.P.G., Harris, J. M., and Whitehouse, R.J.S. (2023). Rock-scour protection of offshore foundations subject to earthquake induced liquefaction, *Ground Engineering*, Dec 2023 Issue, pp. 29–33. Access: https://www.geplus.co.uk/technical-paper/cooling-prize-paper-rock-scour-protection-of-offshore-foundations-subjected-to-earthquake-induced-liquefaction-20-12-2023/

Xu, D.M., Madabhushi, S.P.G., Harris, J. M., and Whitehouse, R.J.S. (2025). On modelling of offshore scour protection rock berms under seismic loading. *Ocean Engineering*, 341(2): 122568. https://doi.org/10.1016/j.oceaneng.2025.122568